

## Intergranular exchange pinning effects in perpendicular recording media

S.J. Greaves, H. Muraoka, Y. Sugita and Y. Nakamura  
RIEC, Tohoku University, Katahira 2-1-1, Aoba ku, Sendai, 980-8577, Japan.

**Abstract**—In a simulation of perpendicular recording media, the exchange coupling between adjacent cells was broken at random to provide domain wall pinning sites. The introduction of such pinning sites can improve the signal/noise ratio of strongly exchange coupled media by reducing the susceptibility of the media to stray fields and thus reducing unwanted erasure of recorded data.

**Index Terms**—Media noise, perpendicular media, pinning sites, recording simulation.

### I. INTRODUCTION

If we consider a recording medium in which the size of the written bits comprises many grains, to maintain a good signal-to-noise ratio some exchange coupling between grains can help to counteract the effects of thermal fluctuations, which act to demagnetise the medium over time. On the other hand, in media with strong exchange coupling between grains a large amount of noise can arise in the output signal from a recorded track due to zig-zag shaped domain wall formation [1],[2]. In this paper we consider the influence of domain wall pinning sites on the transition noise and on the properties of the recorded track, in particular the output and signal/noise ratio for perpendicular recording media.

The magnetisation of discrete cells making up the media was computed using the Landau-Lifshitz-Gilbert equation. The effective field comprised terms for the demagnetising, exchange, anisotropy, external and random fields. The random field terms represent thermal fluctuations and give rise to time dependent phenomena [3]. For the results presented here the waiting time was the same in all cases to allow the results of different simulations to be compared.

The magnetic moments and magnetic fields were resolved into orthogonal components. The direction of magnetisation was represented by a unit vector,  $\mathbf{m}$ , with orthogonal components  $M_x$ ,  $M_y$  and  $M_z$  and the magnitude of saturation magnetisation by a scalar quantity,  $M_s$ . In the model the x-axis component of the exchange field was calculated using

$$H_{ex}(x) = \frac{2A}{M_s} \nabla^2 M_x \quad (1)$$

In (1),  $A$  is the exchange coupling constant. Similar expressions to (1) were used for the y and z exchange field components. For three adjacent cells located on the x-axis and with a separation,  $dx$ , between the centres of the cells (1) becomes [4]

$$H_{ex}(x) = \frac{2A}{M_s} \left( \frac{M_{x-dx} - 2M_x + M_{x+dx}}{dx^2} \right) \quad (2)$$

Exchange breaks between cells were introduced at random to act as domain wall pinning sites. The percentage of exchange breaks was varied from zero (a continuously exchange coupled medium) to 100% (a granular medium). The exchange breaks may be viewed as analogous to segregation of grains, maybe as a result of annealing, varying underlayer thickness etc. The exchange breaks reduce the coupling between cells and act to slow down domain wall movement. To verify this, a single layer medium of thickness 500 Å,  $M_s$  of 300 emu/cc, uniaxial anisotropy,  $K_u$ , of  $1 \times 10^6$  erg/cc perpendicular to the film and  $A$  of  $2.5 \times 10^{-7}$  erg/cm was divided into two regions, one half magnetised upwards and the other half magnetised downwards. After running the simulation for some time a domain wall established itself in the medium. Once the domain wall was stable a 500 Oe field was applied perpendicular to the film and the velocity of the wall calculated as it moved across the medium. Fig. 1 shows the calculated velocities for various percentages of exchange breaks. We find that by the time the density of exchange breaks reaches 40% the domain wall motion is almost completely inhibited. The domain wall velocities in media with low percentages of exchange breaks indicate the susceptibility of these media to stray fields and suggest that written bits may easily be erased by such fields.

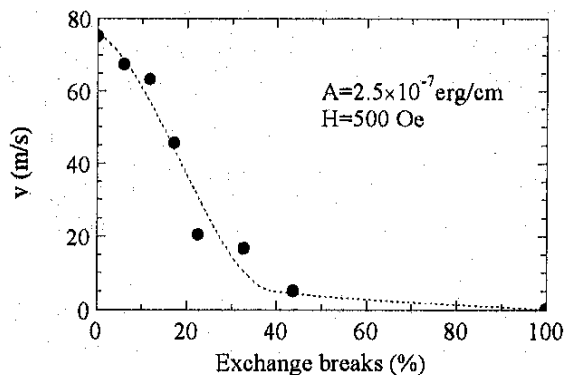


Fig. 1 Domain wall velocity versus percentage of exchange breaks.  $H=500$  Oe.  $A=2.5 \times 10^{-7}$  erg/cm.

Next,  $A$  was increased to  $1 \times 10^{-6}$  erg/cm and a track was written into an initially demagnetised medium at a linear density of 254 kfc. For the writing, field profiles for a shielded single pole head were used. These were derived from the superposition of two ring heads, the field components of which were calculated using the method of

Lindholm [5]. In our approach one head was reversed and offset slightly from the first in order to create the head. In these simulations we used a head width of  $2000\text{\AA}$ , a gap length of  $1000\text{\AA}$  and a pole length of  $400\text{\AA}$ . The head-disc spacing was  $500\text{\AA}$  and the peak perpendicular field during writing was equal to the anisotropy field of the medium ( $6666\text{ Oe}$ ).

## II. RESULTS

Fig. 2(a) shows the written bit pattern in a medium with no exchange breaks. The strong exchange coupling between cells results in the formation of a stripe pattern which barely resembles a written track at all. The introduction of exchange breaks into the medium results in a remarkable change in the written bit pattern. For example, even when the density of exchange breaks is as low as 11.6% (fig. 2(b)), individual bits in the written track can clearly be seen. As the density of exchange breaks increases and the medium becomes subdivided into smaller continuous regions the effect of thermal fluctuations becomes apparent. This can be seen in figs 2(c) and 2(d), in which individual cells within the written bits are seen to have reversed their magnetisation. The recorded track width also decreases as the density of exchange breaks increases since there is less correlation of cell magnetisation in the cross track direction with decreasing exchange

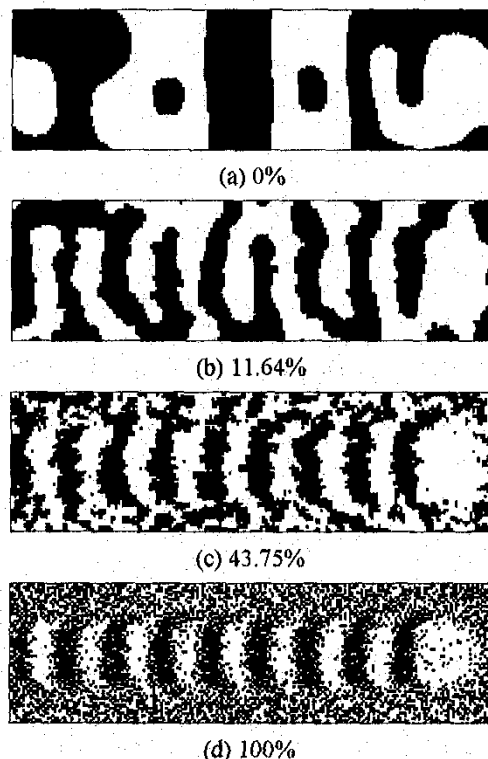


Fig. 2 Written bit patterns for various percentages of exchange breaks. Perpendicular component of  $M$  shown. Black indicates  $M > 0$  and white depicts  $M < 0$ . Depicted images  $0.6\mu\text{m} \times 2\mu\text{m}$ .

coupling. If we compare the written tracks with the location of the exchange breaks we find that the edges of the bits are being pinned at the exchange breaks. This pinning results in rather jagged bit edges for high exchange break densities, e.g. fig. 2(c).

The recorded tracks were analysed by calculating the average magnetisation of pairs of bits along the length of the track. The magnetisation of cells within a track width of  $0.2\mu\text{m}$ , centred on the written track, was included in the averaging. In this way, a profile of the recorded magnetisation for an average bit was built up for each written track. The noise was calculated by comparing the magnetisation profile of each individual bit with that of the average profile for all bits, the deviation from the average profile being the noise. Finally, we calculated the S/N ratio by dividing the area enclosed by the average bit profile by the area under the noise profile.

The average magnetisation profiles of recorded bit-pairs are shown in fig. 3. The recorded bits for a medium with no exchange breaks are non-uniform. However, as exchange breaks are introduced into the medium the bits become uniform and the magnetisation within the bit reaches saturation, as can be seen in the curve for 11.6% exchange breaks in fig. 3. For higher densities of exchange breaks the magnetisation within the bit begins to decrease as isolated cells are created.

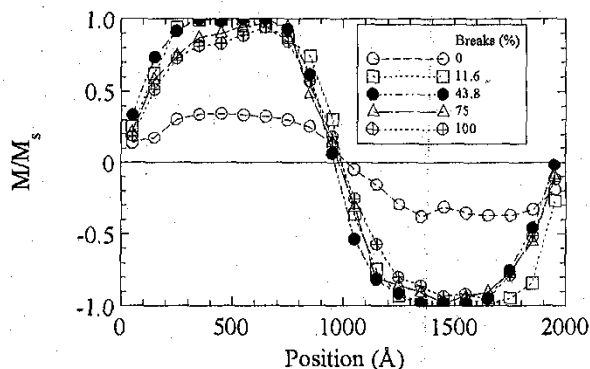


Fig. 3 Average magnetisation for two bits for various percentages of exchange breaks.

Fig. 4 shows the noise for various percentages of exchange breaks. For the exchange coupled medium the noise is large and is distributed at random along the bit length. When exchange breaks are introduced at a low density we find that there is a large decrease in the noise. In addition, the noise becomes concentrated at the bit transitions, around  $M=0$ , as can be seen by a comparison with fig. 3. As the exchange breaks increase further in number, the noise becomes more evenly distributed over the whole bit length.

Fig. 5 shows the signal, noise and signal/noise ratios for various percentages of exchange breaks. We define the signal as the area under the curves shown in fig. 3 and the noise as the area under the curves depicted in fig. 4. We find a peak in the signal for an exchange break density of around

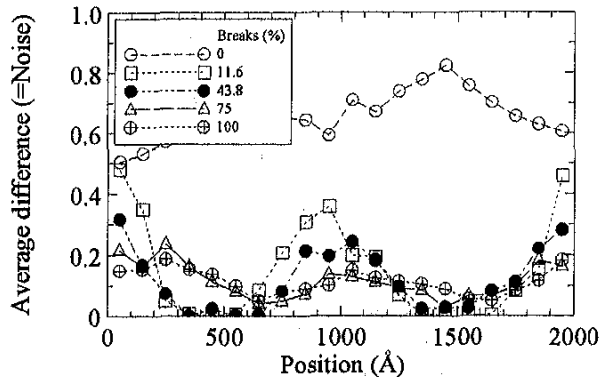


Fig. 4 Noise for two bits for various percentages of exchange breaks.

20%. The noise is very large in the zero exchange break medium but decreases rapidly with the introduction of exchange breaks. The noise level then shows only small variations up to the maximum density of exchange breaks. The signal decreases slowly with increases in the exchange break density above 20% as isolated grains begin to appear in the medium. The signal/noise ratio is a maximum between 20% and 60% density of exchange breaks.

Fig. 6 shows  $\delta M$  curves [6] for media with various percentages of exchange breaks. The remanence curves from which these  $\delta M$  curves were obtained were calculated by applying pulsed fields of  $5.7 \times 10^{-11}$ s duration to the media. We find a range of interactions in the media, from strongly exchange coupled in media with low densities of exchange breaks, to media dominated by magnetostatic interactions at higher exchange break densities. The optimum S/N ratios are obtained when the overall interactions in the medium are a minimum.

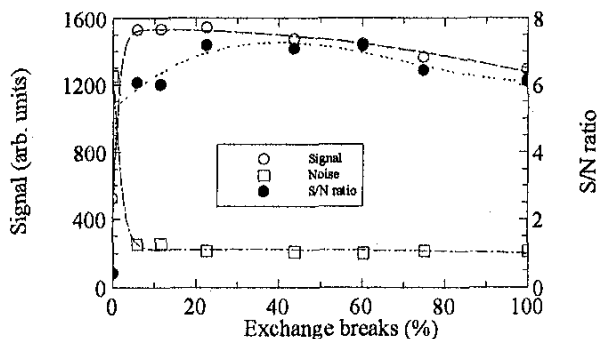


Fig. 5 Signal, noise and S/N ratio versus percentage of exchange breaks for 100Å grain media.

The previous results are all for simulations in which the cell size (grain size) was 100Å. We find similar results, in terms of S/N ratio, for 66Å and 50Å grains and also for recording with a ring head. In each case the optimum S/N ratio is found at around 60% exchange breaks. The overall

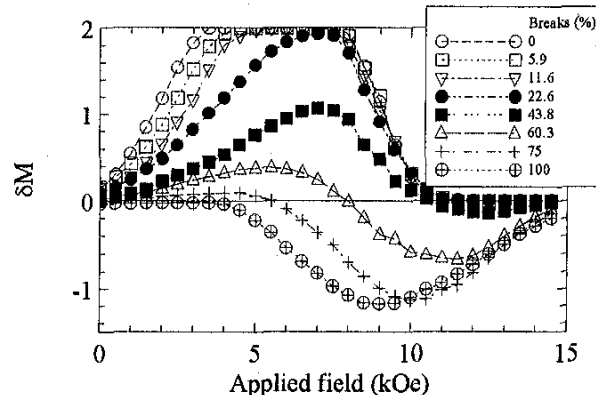


Fig. 6  $\delta M$  curves for various percentages of exchange breaks.

level of interactions, obtained from the areas under the  $\delta M$  curves, are plotted in fig.7 for two grain sizes. We find that the two curves are similar and also that the minima, at about 60% exchange breaks, both coincide with the peak in the S/N ratios.

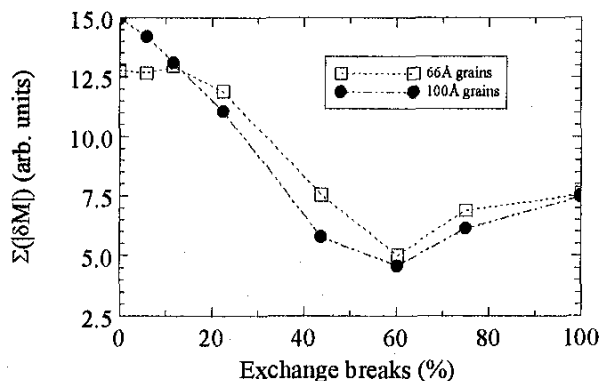


Fig. 7 Area under  $\delta M$  curves versus percentage of exchange breaks for two grain sizes.

### III. CONCLUSIONS

From the results of figs. 5, 6 and 7 we can conclude that aiming to minimise the overall level of interactions in a medium, i.e. the area under the  $\delta M$  curve for that medium, appears to be a useful approach to maximising the S/N ratio.

### REFERENCES

- [1] D.D. Dressler and J.H. Judy, *IEEE Trans. Magn.*, vol. 10, pp. 674-677, 1974.
- [2] H.C. Tong, R. Ferrier, P. Chang, J. Tzeung and K.L. Parker, *IEEE Trans. Magn.*, vol. 20, pp. 1831-1833, 1984.
- [3] W.F. Brown, *IEEE Trans. Magn.*, vol. 15, pp.1196-1208, 1979.
- [4] Y. Nakatani, Y. Uesaka and N. Hayashi, *Jap. J. Appl. Phys.*, vol. 28, pp. 2845-2507, 1989.
- [5] D.A Lindholm, *IEEE Trans. Magn.*, vol. 13, pp.1460-1462, 1977.
- [6] P.E. Kelly, K. O'Grady, P.I. Mayo and R.W. Chantrell, *IEEE Trans. Magn.*, vol. 25, pp. 3881-3883, 1989.